P-ISSN 2586-9000
E-ISSN 2586-9027
Homepage : https://tci-thaijo.org/index.php/SciTechAsia
Science & Technology Asia
Vol. 27 No.3 July - September 2022
Page: [152-174]
Original research article

Development of a Serological Dilution Microfluidic Chip for Immunoassay Applications

Therdthai Thienthong[1], Ekachai Juntasaro[1,*], Numfon Khemthongcharoen[2], Witsaroot Sripumkhai[3], Nongluck Houngkamhang[4], Pattaraluck Pattamang[3], Mayuree Chanasakulniyom[5], Nithi Atthi[3], Chamras Promptmas[2], Panapat Uawithya[6], Wutthinan Jeamsaksiri[3]

[1]*Mechanical Engineering Simulation and Design Group, The Sirindhorn International Thai-German Graduate School of Engineering, King Mongkut's University of Technology North Bangkok, Bangkok 10800, Thailand*
[2]*Department of Biomedical Engineering, Faculty of Engineering, Mahidol University, Nakhon Pathom 73170, Thailand*
[3]*Thai Microelectronics Center, National Electronics and Computer Technology Center, National Science and Technology Development Agency, Chachoengsao 24000, Thailand*
[4]*College of Nanotechnology, King Mongkut's Institute of Technology Ladkrabang, Bangkok 10520, Thailand*
[5]*Department of Clinical Chemistry, Faculty of Medical Technology, Mahidol University, Nakhon Pathom 73170, Thailand*
[6]*Department of Physiology, Faculty of Medicine, Siriraj Hospital, Mahidol University, Bangkok 10700, Thailand*

Received 7 April 2021; Received in revised form 27 February 2022
Accepted 4 March 2022; Available online 29 September 2022

ABSTRACT

This work aims to develop a multiple dilution microfluidic chip that is capable of diluting the human serum by means of two-fold dilution for seven levels from 1:2 to 1:128 with phosphate-buffered saline (PBS) buffer. The dilution in this work is processed in parallel in order to reduce the accumulated errors that the standard pipetting technique generates in the micro-well plate. The serum and PBS buffer are precisely delivered to the micromixers by controlling their flow rates. The dilution is achieved by the passive mixing process for which the serpentine geometry is designed in order to continually generate the Dean vortices along the serpentine microchannel to effectively mix serum and PBS buffer in the microfluidic chip. The prototype of this multiple dilution microfluidic chip is fabricated by using polydimethylsiloxane (PDMS). The dilution-in-parallel capability of this prototype is validated by using the UV-vis absorption method. The results reveal that the measured values

***Corresponding author:** ekachai.j@tggs.kmutnb.ac.th **doi:** 10.14456/scitechasia.2022.53

of the seven dilution ratios obtained are in good agreement with the exact values. Finally, this prototype is evaluated for serological MOG-IgG detection in order to verify the reliable operation of this multiple dilution microfluidic chip. The prototype can successfully detect MOG-IgG at all volume concentration ratios.

Keywords: Dilution; Human serum; Microfluidics; Micromixer; Volume flow rate control network

1. Introduction

Dilution and mixing are widely used in medical diagnostic tests. Numerous medical tests are inevitably involved with human blood, especially serum used as sample for testing. Serum is the plasma without fibrinogen [1]. Both plasma and serum are classified as Newtonian fluid [2] and in general can be dissolved in water. In serum, albumin is the main protein. In the sample preparation, serum is normally diluted by phosphate-buffered saline (PBS) which is a water-based salt solution. PBS buffer is suitable for diluting biological substances because it is isotonic and non-toxic. Conventionally, serum is diluted in a typical 96-microwell plate at multiple concentrations. This commonly used technique needs a skillful technician and a precise tool in order to gain accurately diluted samples, in particular when very low volume concentration is required so that it is cost- and time-consuming. In modern medical tests, the trend is directed towards using a tiny amount of blood/serum leading to very low volume concentration after dilution. A microfluidic chip can play an important role to improve the accuracy and precision of the volume concentration and also to reduce the operation time for both dilution and mixing. Mixing is also another key process in the microfluidic chip [3]. In a micromixer, a sample is mixed with a buffer in order to obtain the homogeneous solution/mixture at outlet. There are several comprehensive reviews on micromixers in the literature [4-7]. In principle, the mixing process in the microfluidic chip can be categorized into two schemes: active and passive. The active mixing scheme requires the external energy or force to generate mixing. The passive mixing scheme induces the chaotic advection [8] by its specifically designed channel in order to increase the contact area and the contact time between the sample and the buffer to enhance mixing. The passive mixing scheme is selected in this work in order to make the microfluidic chip simple, stand-alone and user-friendly without need of any external input. The microchannel in the micromixer is made curved in order to generate the Dean vortex, i.e., a pair of counter-rotating secondary flows over the microchannel cross-section. The Dean vortex, which is one of the effective mechanisms for mixing, can help increase the contact area and the contact time between the sample and the buffer [9]. Recently, the Dean vortex was used to mix the serum with the PBS buffer in the multiple dilution microfluidic chip [10, 11].

Normally a 96-microwell plate is used to dilute serum at multiple concentrations, which requires both skillful technicians and precise tools in order to obtain accurate concentrations, especially at very low volume concentration. Therefore, the 96-microwell plate is cost- and time-consuming. The current demand requires an advanced technique using a tiny amount of serum which can provide very low volume concentration after dilution. In an advanced micromixer, a sample is mixed with a buffer to obtain the homogeneous mixture at the outlet. The benefits of using a multiple dilution microfluidic chip are the reduced amounts of reagents and samples, and the reduction of the turnaround time per test. The objective of the present work is to

develop a stand-alone and user-friendly serological dilution microfluidic chip that is capable of diluting the human serum with the PBS buffer by means of two-fold dilution for seven levels from 1:2 to 1:128 in parallel for immunoassay applications. In this chip, seven micromixers are designed using the serpentine microchannel to induce the Dean vortex for the mixing process. From both serum inlet and PBS inlet to the seven micromixers, the volume flow rate control networks are precisely designed by using Hagen–Poiseuille's law. The prototype is fabricated using polydimethylsiloxane (PDMS) only, which is biocompatible [12, 13]. The dilution-in parallel operation of this prototype is validated by using UV-vis absorption technique. Finally, this prototype is tested for the detection of the Myelin Oligodendrocyte Glycoprotein (MOG-IgG).

2. Design Principle and Procedure

According to the functional block design approach [14], this multiple dilution microfluidic chip has been developed separately into two main functional blocks: the volume flow rate controlling block and the mixing block. Each functional block is developed individually. Then, two functional blocks are connected together to form a complete set of microfluidic microchannel networks. The upstream of this dilution microfluidic chip are the control networks of serum and PBS to deliver the exact amount of serum and PBS to micromixers downstream. Moreover, this chip development is also concerned with some constraints in the multiple dilution microfluidic chip operation. The most serious concern is the number of pumps for operating this multiple dilution chip. The requirement of this development is to use two syringe pumps (one for the serum inlet and the other for the PBS inlet) to deliver seven dilution ratios (two-fold dilution ratios from 1:2 to 1:128) with one negative controlling unit for pure PBS outlet as reference, i.e., eight outlets in total. In this section, there are three main subsections to explain how to design and develop this parallel dilution microfluidic chip: (2.1) for micromixers, (2.2) for volume flow rate control networks and (2.3) for microfabrication of a prototype.

2.1 Design of micromixers

For the development of micromixers, the major difficulty encountered in this work is all about how to mix two fluids into a homogeneous mixture at the micromixer outlet when the flow considered is laminar because the Reynolds number is very low as the microchannel scale is so small. In the laminar flow regime, the molecular diffusion is the main mixing mechanism which is a slow mixing process leading to the lengthy microchannel. The diffusivity can be enhanced by increasing the contact area and the contact time between two fluids. The Dean vortex is chosen to promote the contact area and the contact time between serum and PBS in this work because it is a pair of counter-rotating secondary flows over the cross section of the microchannel. The question is how to generate the Dean vortex. Physically, the Dean vortex is generated by the centripetal force at the bend. Therefore, the micromixer must be made of a continually curved microchannel. The intensity of the Dean vortex is governed by the dimensionless Dean number (Dn) which is defined in Eq. (2.1) The Dean vortex with high intensity takes place when the curvature ratio R_c is low.

$$Dn = \frac{Re}{\sqrt{R/a}} = \frac{Re}{\sqrt{R_c}}\ , \qquad (2.1)$$

$$Re = \frac{Inertial\ force}{Viscous\ force} = \frac{VD_h}{\nu} = \frac{\rho VD_h}{\mu}, \qquad (2.2)$$

where R is the mean radius of curvature, a is the width of the curved microchannel, R_c is the curvature ratio ($R_c = R/a$) which is illustrated in Fig. 1, Re is the Reynolds number, ρ is the fluid density, V is the mean velocity averaged over the cross-sectional area, D_h is the hydraulic diameter of the microchannel, μ is the dynamic viscosity of the fluid and ν is the kinematic viscosity of the fluid ($\nu = \mu / \rho$).

In this work, the Dean vortex is continually generated by the serpentine microchannel as shown in Fig. 1, whose design is obtained by using the constant Dean number with R_c = 1 over the whole length of the micromixer as shown in Fig. 2(b). If the constant Dean number with R_c > 1 is used as shown in Fig. 2(c), i.e. R_c = 2, the intensity of the Dean number will be lower; in other words, mixing is not effective. If the constant Dean number with R_c < 1 is used as shown in Fig. 2(a), i.e., R_c = 0.5, the intensity of the Dean number should be in principle higher but the discontinuous shape will inevitably appear in the design destroying the desired continuous curve.

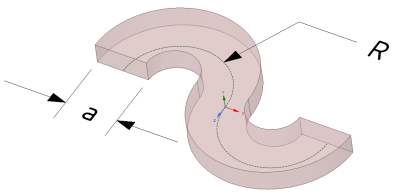

Fig. 1. A serpentine microchannel.

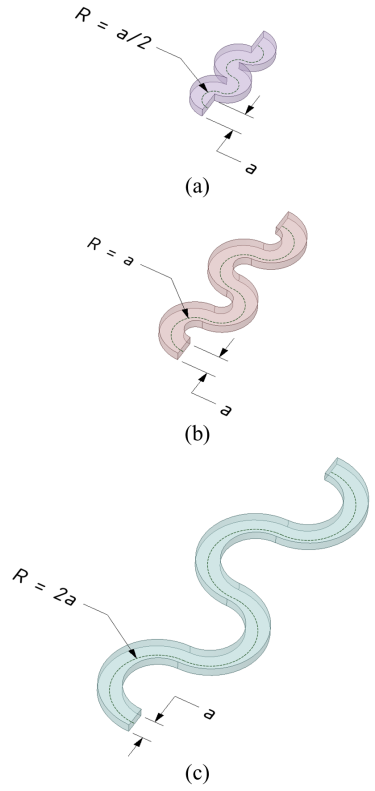

Fig. 2. Serpentine microchannels at various curvature ratios: (a) R_c = 0.5, (b) R_c = 1, and (c) R_c = 2.

In order to create the serpentine microchannel, two major parameters are required: the width of the rectangular cross section a and the mean radius of curvature R, as shown in Fig. 1. The serpentine geometry is mimicked from the study of Thienthong et al. [15, 16]. The serpentine microchannel of this design is an alternating semicircle curved channel connected together in many folds. In this work, the serpentine microchannel consists of 26 quadrants and 56 semicircles connected together. In order to maximize the contact area between serum and PBS, the W-inlet is designed for this micromixer. The serum is fed into the middle inlet while the PBS buffer is fed into the left- and right-side inlets. These inlets are indicated as the PBS inlet 1, the serum inlet 2, and the PBS inlet 3, as shown in Fig. 3. The intersection

angles between the PBS inlet 1 and the serum inlet 2 and also between the PBS inlet 3 and the serum inlet 2 are 45 degrees. This serpentine microchannel has a depth of 40 µm. The three inlets of each serpentine microchannel have the same square cross-section width of 40 µm. As a result, the cross section of the serpentine microchannel is 120 µm wide with R_c equal to 1, and the microchannel path length is 27012 µm (the serpentine curve length is 26012 µm and the straight length is 1000 µm). The geometry and dimension of one micromixer unit are shown in Fig. 3.

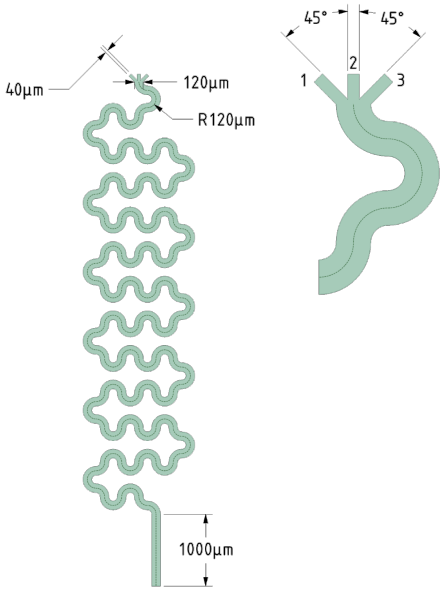

Fig. 3. Geometry and dimension of a micromixer unit.

In order to operate seven micromixers as designed for delivering the volume concentration ratios from 1:2 to 1:128, the volume flow rate of each inlet must be specified. By maintaining the same volume flow rate of mixture (Q_{mix}) at the outlets of all micromixers, the volume flow rates of serum and PBS can be determined and hence controlled. Since Q_{mix} is prescribed as a constant for all volume concentration ratios, the volume flow rate of mixture can be expressed as

$$Q_{mix} = Q_s + Q_p, \tag{2.3}$$

where Q_s is the volume flow rate of serum and Q_p is the volume flow rate of the PBS buffer. The relation between the volume concentration of serum (ϕ_s) and that of PBS buffer (ϕ_p) is given as

$$\phi_s + \phi_p = 1. \tag{2.4}$$

Then, multiplying Eq. (2.4) by Q_{mix} gives

$$\phi_s Q_{mix} + \phi_p Q_{mix} = Q_{mix}. \tag{2.5}$$

Matching Eq. (2.5) with Eq. (2.3) yields

$$\begin{aligned} Q_s &= \phi_s Q_{mix}, \\ Q_p &= \phi_p Q_{mix}. \end{aligned} \tag{2.6}$$

For example, given ϕ_s = 1/64 and the constant Q_{mix} = 128 [µL/min]. Hence, Q_s = (1/64)×128 = 2 [µL/min] and Q_p = (63/64)×128 = 126 [µL/min]. In this study, the serum and PBS volume flow rates of various volume concentration ratios are calculated based on Eq. (2.6) as summarized in Table 1.

Table 1. Volume flow rates of serum and PBS at the inlets of micromixers.

Volume concentration ratio	Volume flow rate at inlet [µL/min]		
	PBS inlet 1	Serum inlet 2	PBS inlet 3
1:2	32	64	32
1:4	48	32	48
1:8	56	16	56
1:16	60	8	60
1:32	62	4	62
1:64	63	2	63
1:128	63.5	1	63.5

After the geometry and dimension of micromixers and the volume flow rates of serum and PBS required at micromixer inlets are obtained, the next task is to evaluate the mixing performance of this micromixer design. Since the micromixer outlet is only 120 μm wide, it is difficult by means of experiment to quantitatively measure the homogeneity of the mixture at the outlet. The numerical simulation is used instead to predict the mixture of serum and PBS at the micromixer outlet and then the mixing index is used to quantify the homogeneity level of the predicted mixture at the outlet. In this work, the mixing index (MI) defined in Eq. (2.7) is used to evaluate the mixing performance.

$$MI = 1 - \frac{\sum_{i=1}^{N}\left[| \phi_i - \overline{\phi_a} | A_i \right]}{2 | \overline{\phi_a} | \sum_{i=1}^{N} A_i}, \tag{2.7}$$

where ϕ_i is the local volume concentration at the i^{th} cell, A_i is the cross-sectional area of the i^{th} cell, $\overline{\phi_a}$ is the area-weighted average of volume concentration at the cross-sectional area which is defined as

$$\overline{\phi_a} = \frac{\sum_{i=1}^{N} \phi_i A_i}{\sum_{i=1}^{N} A_i}. \tag{2.8}$$

In this work, the commercial CFD software ANSYS FLUENT version 18.2 is used to simulate the serum, PBS and mixture flows inside micromixers and its results at the micromixer outlet are used to calculate MI in order to evaluate the level of homogeneity of the mixture. In simulation, three governing equations are required: continuity, species transport and Navier Stokes equations. The governing equations are simplified based on the following assumptions: (1) serum, PBS and mixture are the Newtonian fluids, (2) the fluid flow is steady, incompressible and laminar, (3) there is no chemical reaction between serum and PBS, (4) the diffusivity between serum and PBS is identical due to the binary mixture process [17]. Thus, three governing equations can be written as follows:

Continuity equation:

$$\frac{\partial(\rho u)}{\partial x} + \frac{\partial(\rho v)}{\partial y} + \frac{\partial(\rho w)}{\partial z} = 0, \tag{2.9}$$

where u, v, and w are the velocity components in the x-, y- and z-directions of the Cartesian coordinate system, respectively, and ρ is the density of mixture.

Species transport equation for serum and PBS:

$$\frac{\partial(\rho u \omega_s)}{\partial x} + \frac{\partial(\rho v \omega_s)}{\partial y} + \frac{\partial(\rho w \omega_s)}{\partial z} = -\left(\frac{\partial j_{s,x}}{\partial x} + \frac{\partial j_{s,y}}{\partial y} + \frac{\partial j_{s,z}}{\partial z}\right), \tag{2.10}$$

$$\frac{\partial(\rho u \omega_p)}{\partial x} + \frac{\partial(\rho v \omega_p)}{\partial y} + \frac{\partial(\rho w \omega_p)}{\partial z} = -\left(\frac{\partial j_{p,x}}{\partial x} + \frac{\partial j_{p,y}}{\partial y} + \frac{\partial j_{p,z}}{\partial z}\right), \tag{2.11}$$

where ω_s and ω_p are the mass fractions of serum and PBS, respectively, j_s is the mass diffusion flux of serum and j_p is the mass diffusion flux of PBS which can be described based on the Cartesian coordinate system in the following equations.

Mass diffusion flux of serum (j_s):

$$j_{s,x} = -\mathcal{D}_{sp} \frac{\partial(\rho \omega_s)}{\partial x},$$

$$j_{s,y} = -\mathcal{D}_{sp} \frac{\partial(\rho \omega_s)}{\partial y},$$

$$j_{s,z} = -\mathcal{D}_{sp} \frac{\partial(\rho\omega_s)}{\partial z}. \quad (2.12)$$

Mass diffusion flux of PBS (j_p):

$$j_{p,x} = -\mathcal{D}_{ps} \frac{\partial(\rho\omega_p)}{\partial x},$$
$$j_{p,y} = -\mathcal{D}_{ps} \frac{\partial(\rho\omega_p)}{\partial y}, \quad (2.13)$$
$$j_{p,z} = -\mathcal{D}_{ps} \frac{\partial(\rho\omega_p)}{\partial z},$$

where $\mathcal{D}_{sp}$ and $\mathcal{D}_{ps}$ are the diffusion coefficients of serum and PBS [cm^2/s], respectively, which are identical [17] ($\mathcal{D}_{sp} = \mathcal{D}_{ps}$). This $\mathcal{D}_{sp}$ of binary liquids can be calculated by using the following formula [18]:

$$\mathcal{D}_{sp} = 7.4\times10^{-8} \frac{\sqrt{\psi_p M_p}T}{\mu \tilde{V}_s^{0.6}}, \quad (2.14)$$

where ψ_p is the association parameter for PBS ($\psi_p = 2.6$) [18], M_p is the molecular weight of PBS [g/mol], T is the absolute temperature [K], $\tilde{V}_s$ is the molar volume of the serum [cm^3/mol] and μ is the viscosity of mixture [mPa-s].

Navier-Stokes equations:

$$\frac{\partial(\rho uu)}{\partial x} + \frac{\partial(\rho vu)}{\partial y} + \frac{\partial(\rho wu)}{\partial z} = -\frac{\partial p}{\partial x} + [\frac{\partial}{\partial x}\tau_{xx} + \frac{\partial}{\partial y}\tau_{yx} + \frac{\partial}{\partial z}\tau_{zx}], \quad (2.15)$$

$$\frac{\partial(\rho uv)}{\partial x} + \frac{\partial(\rho vv)}{\partial y} + \frac{\partial(\rho wv)}{\partial z} = -\frac{\partial p}{\partial y} + [\frac{\partial}{\partial x}\tau_{xy} + \frac{\partial}{\partial y}\tau_{yy} + \frac{\partial}{\partial z}\tau_{zy}], \quad (2.16)$$

$$\frac{\partial(\rho uw)}{\partial x} + \frac{\partial(\rho vw)}{\partial y} + \frac{\partial(\rho ww)}{\partial z} = -\frac{\partial p}{\partial z} + [\frac{\partial}{\partial x}\tau_{xz} + \frac{\partial}{\partial y}\tau_{yz} + \frac{\partial}{\partial z}\tau_{zz}], \quad (2.17)$$

where p is the pressure and τ_{ij} is the viscous stress terms which can be defined as follows:

$$\tau_{xx} = 2\mu[\frac{\partial u}{\partial x}] - \frac{2}{3}\mu[\frac{\partial u}{\partial x} + \frac{\partial v}{\partial y} + \frac{\partial w}{\partial z}], \quad (2.18)$$

$$\tau_{yy} = 2\mu[\frac{\partial v}{\partial y}] - \frac{2}{3}\mu[\frac{\partial u}{\partial x} + \frac{\partial v}{\partial y} + \frac{\partial w}{\partial z}], \quad (2.19)$$

$$\tau_{zz} = 2\mu[\frac{\partial w}{\partial z}] - \frac{2}{3}\mu[\frac{\partial u}{\partial x} + \frac{\partial v}{\partial y} + \frac{\partial w}{\partial z}], \quad (2.20)$$

$$\tau_{xy} = \tau_{yx} = \mu[\frac{\partial v}{\partial x} + \frac{\partial u}{\partial y}], \quad (2.21)$$

$$\tau_{yz} = \tau_{zy} = \mu[\frac{\partial w}{\partial y} + \frac{\partial v}{\partial z}], \quad (2.22)$$

$$\tau_{zx} = \tau_{xz} = \mu[\frac{\partial u}{\partial z} + \frac{\partial w}{\partial x}]. \quad (2.23)$$

In this work, the density and viscosity of fluids are measured by using the Density Meter DMA4500M, Anton Paar GmbH, and the Automated Micro Viscometer (AMVn), Anton Paar GmbH, respectively. The density and viscosity of serum, PBS buffer and mixtures at different volume concentration ratios are given in Table 2.

Table 2. Measured mechanical properties of serum, PBS buffer and mixtures at different volume concentration ratios.

Samples	Viscosity [mPa·s]	Density [g/cm^3]
PBS	0.92558	1.00367
1:128	0.94178	1.00376
1:64	0.95090	1.00395
1:32	0.97260	1.00398
1:16	1.00010	1.00489
1:8	1.03110	1.00624
1:4	1.07370	1.00872
1:2	1.21406	1.01416
Serum	1.65578	1.02468

The diffusion coefficients are independently obtained for each volume concentration ratio based on Eq. (2.14) as

shown in Table 3. These diffusion coefficients remain constant along the flow path. In this study, the association parameter for PBS (ψ_p) is specified as 2.6 [18], the molecular weight of PBS (M_p) is 411.029 [g/mol] obtained from the National Center for Biotechnology Information [19]. According to the temperature of the testing and measuring conditions, T is equal to 298.15 [K]. The molar volume of the serum $\tilde{V}_s$ is equal to 64836.827 [cm^3/mol] which is calculated from the molecular weight of serum (M_s = 66437 [g/mol], referred to the molecular weight of the majority protein in the serum [20]) divided by its density (as shown in Table 2). The viscosities of mixtures (μ_{mix}) are shown in Table 2.

Table 3. Diffusion coefficients between serum and PBS buffer at various volume concentration ratios.

Volume concentration ratio	$\mathcal{D}_{sp}$ [cm^2/s]
1:128	9.9322E-07
1:64	9.8370E-07
1:32	9.6175E-07
1:16	9.3530E-07
1:8	9.0718E-07
1:4	8.7119E-07
1:2	7.7047E-07

Since the viscosity of serum is almost two times higher than the viscosity of PBS, as shown in Table 2, and the volume flow rates of serum and PBS required at the micromixer inlets are different at each volume concentration ratio, as shown in Table 1, the pressure drop must be balanced by using Hagen–Poiseuille's law [21] in order to deliver both serum and PBS to the micromixer inlets at the same time. The pressure drop (Δp) is formulated as follows [21]:

$$\Delta p = 12\mu Q \frac{L}{ba^3} \frac{1}{\left[1 - \frac{192a}{\pi^5 b} \sum_{i=1,3,5,\ldots}^{\infty} \frac{\tanh(i\pi b / 2a)}{i^5}\right]}, \quad (2.24)$$

where μ is the dynamic viscosity of fluid, Q is the volume flow rate, L is the length of the microchannel, a is the width of the microchannel cross section, and b is the height of the microchannel cross section. Since three inlets of one micromixer have the same cross-sectional area, the ratio of the PBS-inlet pressure drop to the serum-inlet pressure drop can be calculated by using the following simplified equation:

$$\frac{\Delta p_p}{\Delta p_s} = \frac{\mu_p Q_p L_p}{\mu_s Q_s L_s}, \quad (2.25)$$

where Δp_p and Δp_s are the PBS-inlet and serum-inlet pressure drops, μs and μp are the viscosities of serum and PBS, Q_s and Q_p are the volume flow rates of serum and PBS, and L_s and L_p are the lengths of serum and PBS inlets. When the pressure drop is balanced, i.e., $\Delta p_p / \Delta p_s = 1$, it yields

$$\frac{L_s}{L_p} = \frac{\mu_p Q_p}{\mu_s Q_s}. \quad (2.26)$$

Eq. (2.26) gives the ratio of the serum-inlet length to the PBS-inlet length for the CFD simulation of flow inside micromixers in order to numerically evaluate the mixing performance of micromixers. Table 4 provides the lengths of both serum and PBS inlets.

Table 4. Lengths of seven individual micromixer inlets.

Volume concentration ratio	PBS inlet length [μm]	Serum inlet length [μm]
1:128	125	4437
1:64	125	2201
1:32	125	1083
1:16	125	524
1:8	125	244
1:4	125	104
1:2	250	69

Fig. 4 illustrates the micromixers of seven volume concentration ratios with the

appropriate lengths of both the serum and PBS inlets obtained in Table 4.

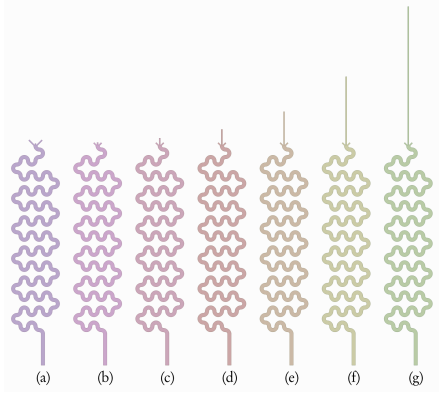

Fig. 4. Micromixers of seven volume concentration ratios: (a) 1:2, (b) 1:4, (c) 1:8, (d) 1:16, (e) 1:32, (f) 1:64, (g) 1:128.

For CFD simulation, the symmetry boundary condition is applied at the half height of the microchannel so that the height of the flow domain is reduced to 20 μm. The mesh is generated by using the sweep mesh method in ANSYS meshing tool and hexahedral and prism elements are chosen for this work. There are 16 elements along the microchannel depth and 32 elements across each inlet width so that there are 96 elements across the microchannel width of the micromixer. With this structured mesh, the high-quality of mesh is obtained as indicated by aspect ratio, skewness and orthogonality in Table 5.

Table 5. Mesh information.

		Volume Concentration Ratio						
		1:2	1:4	1:8	1:16	1:32	1:64	1:128
	Number of elements	26,536,112	26,447,952	26,505,296	26,619,984	26,848,848	27,307,088	28,222,544
Aspect Ratio "Aspect Ratio = 1" is perfect.	Min	1						
	Max	4.5685						
	Average	1.3591						
Skewness "Skewness = 0" is perfect.	Min	0						
	Max	0.51843						
	Average	0.0040125						
Orthogonal Quality "Orthogonal Quality = 1" is perfect.	Min	0.56616						
	Max	1						
	Average	0.99989						

For CFD simulation, the SIMPLEC algorithm is used for the pressure-velocity coupling scheme. The spatial discretization schemes of gradient, pressure and momentum are performed by using the least squares cell based, second order and second order upwind schemes, respectively. The species transport model is setup based on the constant mass diffusion coefficient in this simulation as given in Table 3. The numerical solutions of all volume concentrations ratios converge at the residuals lower than 1.0e-5.

The flow conditions used for CFD simulations at seven volume concentration ratios are taken from Table 1, where the volume flow rates are converted to the mass flow rates and then used as the inlet boundary conditions at both serum and PBS inlets. For the boundary conditions at the micromixer outlets, the atmospheric pressure is applied, i.e., P_{atm} = 0 Pa. The simulation results are used to calculate the values of *MI* using Eq. (2.7) at various locations along the flow path in order to monitor the mixture homogeneity from the inlet to the outlet of micromixer as shown in Fig. 5.

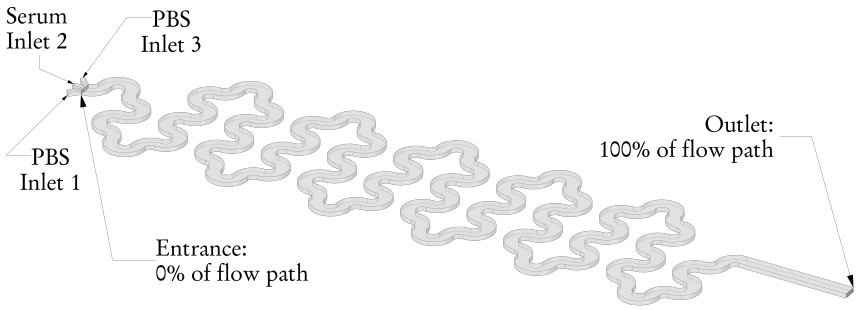

Fig. 5. Flow path length of the serpentine micromixer.

Fig. 6 shows the computed results of the mixing index obtained at the outlets of seven micromixers from 1:128 (0.78125%) to 1:2 (50%) volume concentration ratios. It is found that the current design of the micromixer can provide the homogeneous mixture at the micromixer outlets up to the minimum mixing index of 0.96328 for the volume concentration ratio of 1:2 (50%) and the maximum mixing index of 0.98399 at the volume concentration ratio of 1:64 (1.5625%). The mixing index is more or less constant over a range of 0.78125%-3.125% at MI = 0.984 and then decreases with increasing volume concentration ratio.

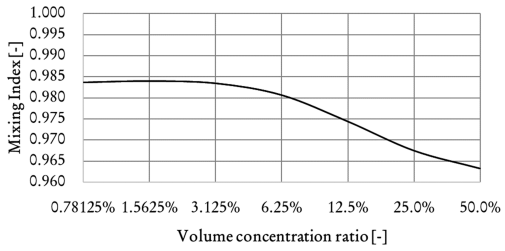

Fig. 6. Mixing index obtained at the micromixer outlet at various volume concentration ratios.

Fig. 7 demonstrates the variation of the mixing index along the flow path of the micromixer from the inlet to the outlet of the micromixer which indicates how much the mixture becomes homogeneous along the flow path of the micromixer. The mixing index starts off with lower value at lower volume concentration ratio: MI = 0.13695 at volume concentration ratio of 1:128 and MI = 0.52081 at volume concentration ratio of 1:2. The mixing index increases rapidly during the first 20% of the flow path length and then becomes constant during the 20% - 30% of the flow path length, except for the volume concentration ratios of 1:2 (constant up to 45% of the flow path length), 1:4 (continue increasing with lower rate) and 1:8 (continue increasing with lower rate). After that, the mixing index keeps increasing and asymptotically approaches the maximum value at the micromixer outlet.

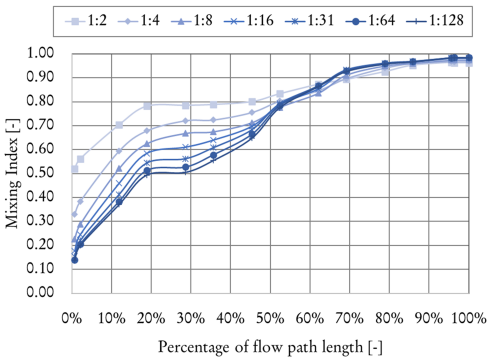

Fig. 7. Mixing index obtained at the micromixer outlet at various volume concentration ratios.

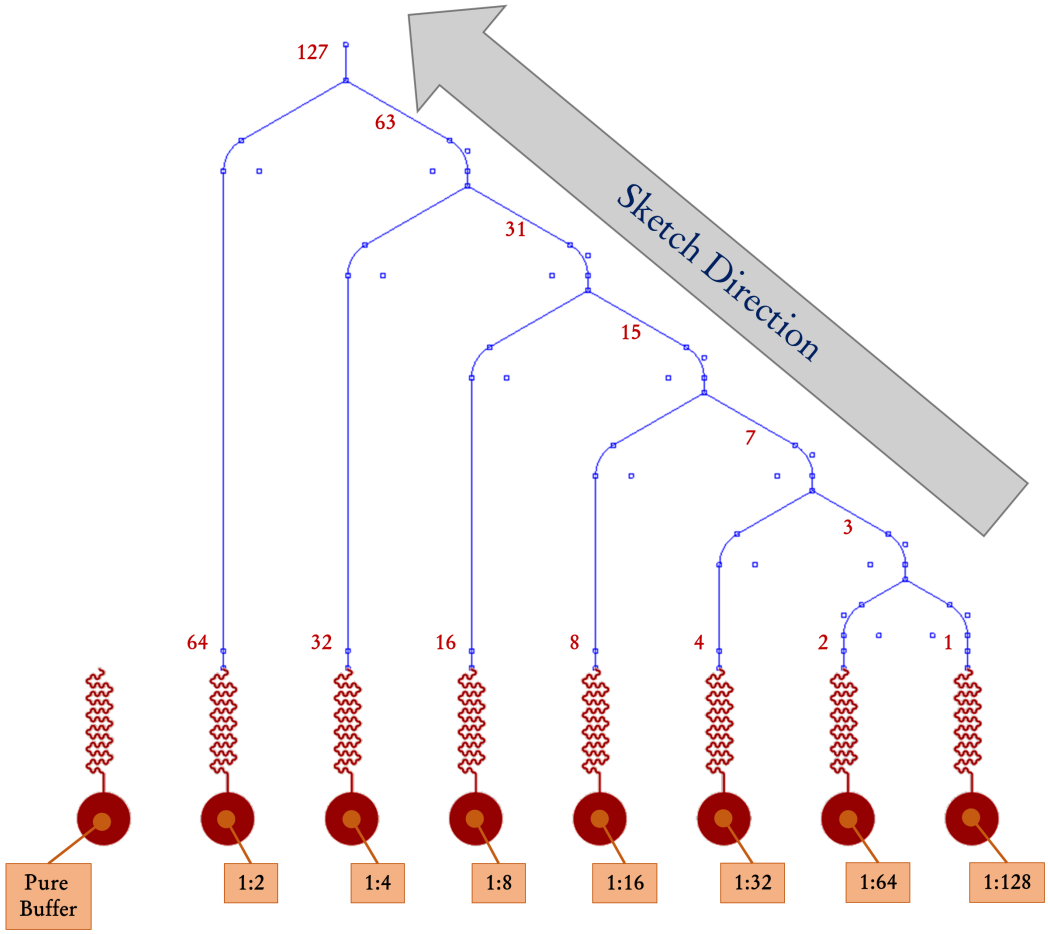

Fig. 8. Sketch of the serum network with the volume flow rate of each microchannel section [μL/min].

2.2 Design of volume flow rate control networks

To deliver the accurate and precise amount of serum and PBS to seven micromixers, two volume flow rate control networks for serum and PBS are analytically designed based on Hagen–Poiseuille's law [21]. According to the conservation laws of mass and momentum, the pressure drop (Δp) along the microchannel with a rectangular cross-section is a function of the volume flow rate, the cross-sectional width, the cross-sectional height, the fluid viscosity and the microchannel length as shown in Eq. (2.24). Over each branch of the microchannel network, the pressure drop between the inlet and the outlet must be equal to that of other branches.

There are two volume flow rate control networks for serum and PBS. The first network of serum consists of one serum inlet and seven outlets to micromixers. The second network of PBS is composed of one PBS inlet and fourteen outlets to micromixers, together with three extra outlets for the reference micromixer. The reference micromixer is used for monitoring the background noise while measuring the fluorescence intensity. In other words, the reference micromixer is used for the negative control where a particular sample is included in the experiment and treated like all the other samples but not expected to change due to any variable in the experiment. Besides the reference micromixer, the number of PBS outlets is

two times higher than the number of serum outlets because PBS is designed to enter each micromixer from left and right sides of the serum inlet at the angle of 45° with respect to the serum inlet in order to enhance mixing [15]. The pressure drops of both networks must be equal and balanced separately. The first step of the design of both volume flow rate control networks is to sketch both networks from the outlet to the inlet in order to obtain the total length of the microchannel used in each branch with consideration of the microfabrication limitation. The challenge of this development is that this 7-dilution microfluidic chip should fit in a square area of 90 mm which is a maximum size for the fabrication using the 6-inch diameter wafer. Moreover, the working radius for the outlet pads should be at least 1.5 mm each in order to connect them with the silicone tubes without any damage to the chip. The minimum distance from one microchannel side wall to another should be more than 150 μm apart. This distant gap allows the sufficient bonding forge between a PDMS cavity and a PDMS substrate to prevent the delamination during the chip operation. The microfabrication will be described in detail in Subsection 2.3. To obtain the precise length of the microchannel in each branch, eight micromixers (including the reference micromixer) with outlet pads are laid out evenly in the layout. After that, the volume flow rate control networks of serum and PBS are sketched. For the serum network, the microchannel sketch starts from a pair of the 1:128 branch and the 1:64 one because their microchannel widths are expected to be very small for a tiny amount of serum at this very low volume concentration ratios so that their microchannel lengths are enforced to be rather short to keep the friction as low as possible; otherwise, the narrow microchannel with long length inevitably generates tremendous friction. For each pair of two neighboring branches, their microchannel sketch is made symmetrical. This sketching pattern is applied further to all higher volume concentration ratios from the 1:32 branch towards the 1:2 one. The largest microchannel width is expected to take place in the 1:2 branch with long length without too much friction. The whole sketch of the serum network is shown in Fig. 8 in which the volume flow rate of each microchannel section is given.

The microchannel sketch of the PBS network is designed in a manner of the symmetrical pattern because PBS is distributed almost uniformly to the fourteen outlets to seven micromixers, together with the extra three outlets to the reference micromixer as shown in Fig. 9 in which the volume flow rate of each microchannel section is given. Again, the sketch is drawn starting from the outlet to the inlet of PBS. To avoid the intersection of the PBS network with the serum network, the PBS network is placed on the opposite side of the serum network. At this point, both serum and PBS networks can be integrated together in combination with seven micromixers and one extra micromixer for reference as shown in Fig. 10.

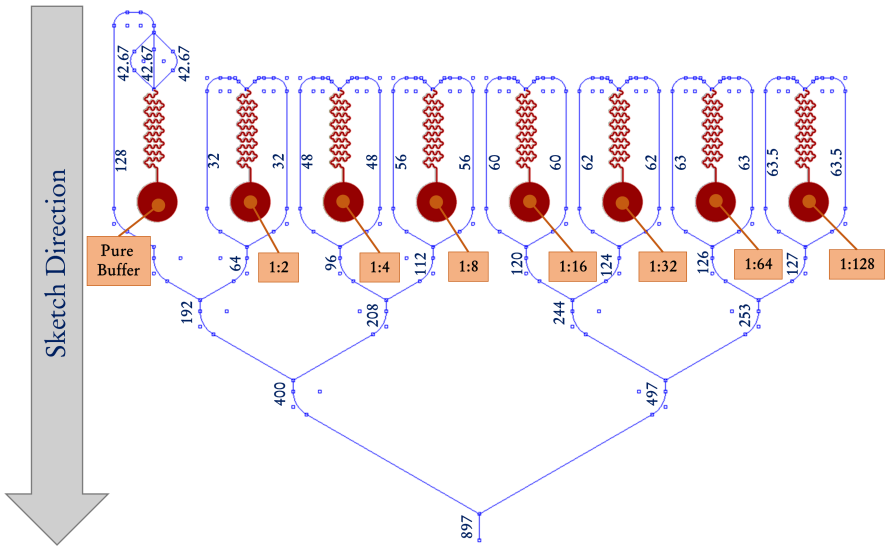

Fig. 9. Sketch of the PBS network with the volume flow rate of each microchannel section [μL/min].

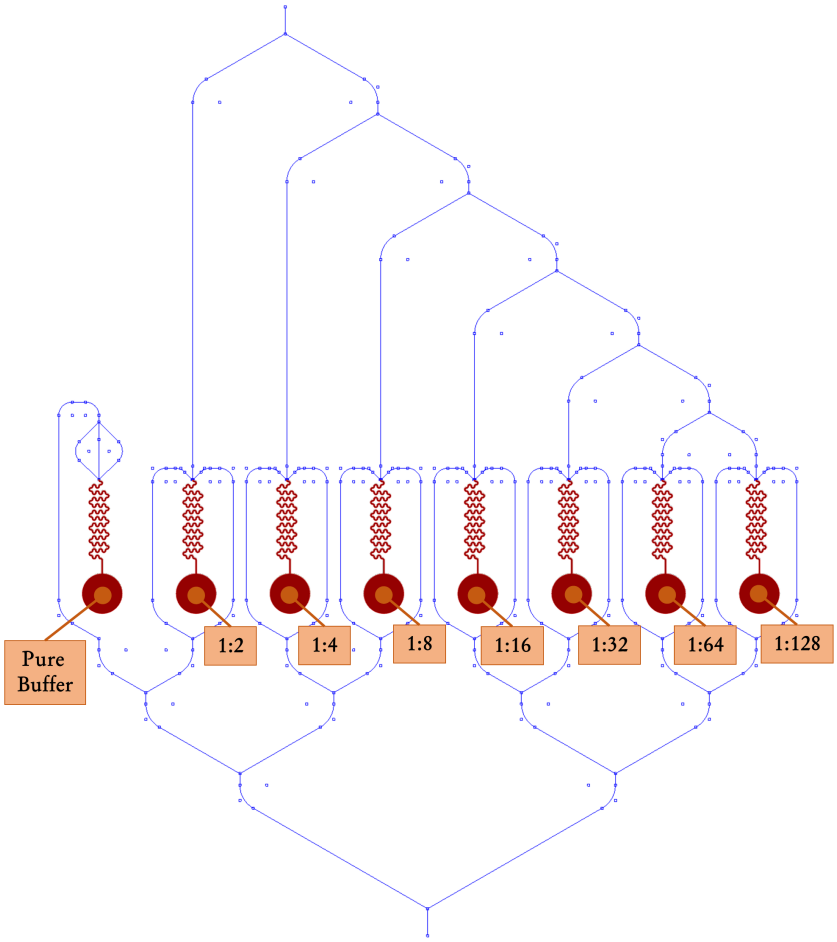

Fig. 10. Combination of serum and PBS networks with micromixers.

After a complete sketch of serum and PBS networks is obtained, the length of each branch can be used in the pressure drop formulation in order to determine the width of each branch because the pressure drop of all branches is equal and the depth of all branch microchannels of serum and PBS networks is equal and specified to be 40 μm.

Up to now, according to Eq. (2.24), the volume flow rate, the depth of the microchannel (or the cross-sectional height), the fluid viscosity and the microchannel length are known but both the cross-sectional width and the pressure drop are still unknown. In order to determine the cross-sectional widths of all branches in the serum and PBS networks, one typical/common pressure drop must be specified into Eq. (2.24). In this work, the 1-μL/min branch is selected to determine such a common pressure drop because this branch is shortest and delivers the lowest volume flow rate of serum to the 1:128 micromixer, i.e., only 1 μL/min. As a result, the microchannel with a square cross section (40 μm wide and 40 μm deep) is specified for the 1- μL/min branch because the square cross section provides the lowest friction and hence shorter time for operation and avoids the mechanical damage due to accumulated pressure within the chip while operation.

After the pressure drop of the 1-μL/min branch is determined, which is 1787.17 Pa, the pressure drop of the 2-μL/min branch must be equal to that of the 1-μL/min one in order to deliver the serum to the inlets of the 1:64 and 1:128 micromixers at the same time. With the pressure drop of the 1-μL/min branch, the cross-sectional width of the 2-μL/min branch can be determined from Eq. (2.24). At this point, the cross-sectional width of the 3-μL/min branch above can be obtained directly by adding the cross-sectional widths of the 1-μL/min and 2-μL/min branches together. Then, the pressure drop of the 3-μL/min branch can be determined from Eq. (2.24). Now the pressure drop of the 4-μL/min branch is equal to a summation of the pressure drop of the 3-μL/min branch with the 1-μL/min one and hence the cross-sectional width of the 4-μL/min branch can then be determined from Eq. (2.24). This calculation procedure can be repeated up to the 64-μL/min branch. Finally, the cross-sectional width of the 127-μL/min branch can be obtained. This calculation procedure is for the serum network.

For the PBS network, it is designed in a similar way. To begin with, the pressure drop of a single 42.67-μL/min branch of the reference micromixer on the far left of the PBS network in Fig. 9 is set to be equal to the pressure drop of the 1-μL/min branch of the serum network. Then, the cross-sectional width of the single 42.67-μL/min branch can be determined from Eq. (2.24). A summation of three 42.67-μL/min branches provides the cross-sectional width of the 128-μL/min branch which then can be used to determine the pressure drop of the 128-μL/min branch using Eq. (2.24). At this point, either the left or the right PBS branch to enter each micromixer from 1:2 to 1:128 has the same pressure drop which is equal to a summation of the 128-μL/min-PBS-branch pressure drop and the 1-μL/min serum-branch pressure drop. Then, the cross-sectional widths of all left and right inlets to all micromixers can be determined from Eq. (2.24). After that, the cross-sectional width of the 127-μL/min PBS branch is equal to a summation of the cross-sectional widths of the left and right PBS branches of the 1:128 micromixer. This kind of cross-sectional width summation can be done repeatedly up to the 897-μL/min branch, or the PBS inlet.

However, the connection between the volume flow rate networks and the micromixers is not straightforward because the outlet widths of the serum and PBS networks are larger than the inlet widths of the micromixers: 40 - 960 μm wide for the serum-network outlets, 114 - 276 μm wide

for the PBS-network outlets and 40 μm wide for the micromixer inlets. The direct connection between a larger outlet to a smaller inlet causes the recirculation zone at their interface which is one type of the minor loss causing the pressure drop in the piping system. The minor loss cannot be eliminated but can be reduced by using a proper fitting at their interface. In this work, a nozzle is employed to reduce the minor loss. Fig. 11 shows a typical nozzle used. However, Hagen–Poiseuille's law in Eq. (2.24) used to design the serum and PBS networks cannot be used to design the nozzle. CFD simulation is used to determine the pressure drop of each nozzle connecting the network outlet to the micromixer inlet.

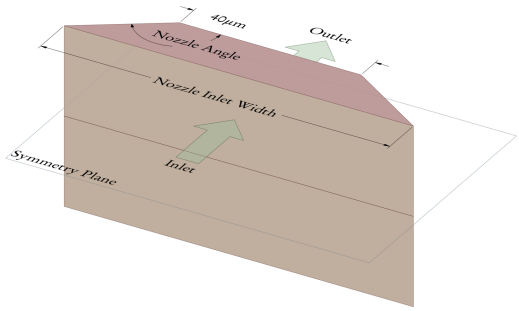

Fig. 11. Domain geometry of a typical nozzle.

For CFD simulation, the ANSYS FLUENT 18.2 software is employed. For the simulation of steady three-dimensional laminar flow through the nozzle, the SIMPLEC algorithm is used for the pressure-velocity coupling scheme. The spatial discretizations of gradient, pressure and momentum are calculated by using the least squares cell-based, second order and second order upwind schemes respectively. Half of the nozzle domain is considered because the fluid domain is symmetrical with respect to the symmetry plane which is located in the middle between the top and bottom walls of the nozzle as shown in Fig. 11. The fluid domain is meshed with hexahedral by using the sweep mesh method in ANSYS meshing tool. There are typically 16 elements across the half height of each nozzle and 32 elements across the width of each nozzle.

The density and viscosity of serum and PBS given in Table 2 are applied in the CFD simulation. The parametric study is used here to find the optimal nozzle geometry that provides the minimum pressure drop. The input parameters consist of (1) 6 microchannel widths from the serum network as discrete parameters, (2) 9 microchannel widths from the PBS network as discrete parameters, (3) one nozzle outlet width of 40 micron as a fixed constant, and (4) the nozzle angles from 93 to 165 degrees with 2 degrees increment. The combination of these four parameters generates 222 simulation cases for the serum nozzle geometry and 333 simulation cases for the PBS nozzle geometry.

This parametric study results in the pressure drop chart across the nozzle as shown in Fig. 12. In order to obtain an optimal nozzle geometry that can be commonly applied over a wide range of this multiple dilution from 1:2 to 1:128 and also can fit a new design or redesign of the serum and PBS networks in the future, the nozzle angle of 147 degrees is chosen for those purposes because at this nozzle angle its root-mean-square error (RMSE) is found to be a minimum in comparison with that of other nozzle angles from 93 to 165 degrees as shown in Fig. 13. This minimum RMSE implies that the difference between the averaged pressure drop and the individual pressure drop of each nozzle is lowest. The nozzle with the optimal nozzle angle of 147 degrees is used to connect all the nozzle inlets from both serum and PBS networks to 8 micromixers.

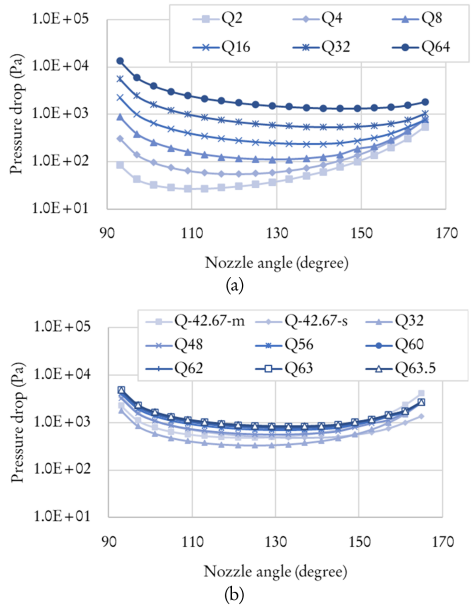

Fig. 12. Pressure drop across (a) the serum nozzle and (b) the PBS nozzle.

However, as indicated in Fig. 12(a) and 12(b) for both serum and PBS networks respectively, the pressure drop across the nozzle of each branch is different even though the optimal nozzle angle of 147 degrees is used. The pressure drop from the nozzle outlet to the micromixer inlet must be balanced by using Eq. (2.24) but this time the microchannel length from the nozzle outlet to the micromixer inlet, called the extended length, is the unknown variable that needs to be determined. Since the largest change of the microchannel width from two volume flow rate control networks to eight micromixer occurs across the 64-μL/min serum nozzle, its pressure drop is thus highest and its extended length must be determined first by using Eq. (2.24). Then, Eq. (2.24) is used to find the extended length for others by using the pressure drop difference between the 64-μL/min serum nozzle and the nozzle of interest. Finally, a prototype of the multiple dilution microfluidic chip can be analytically and numerically obtained as shown in Fig. 14.

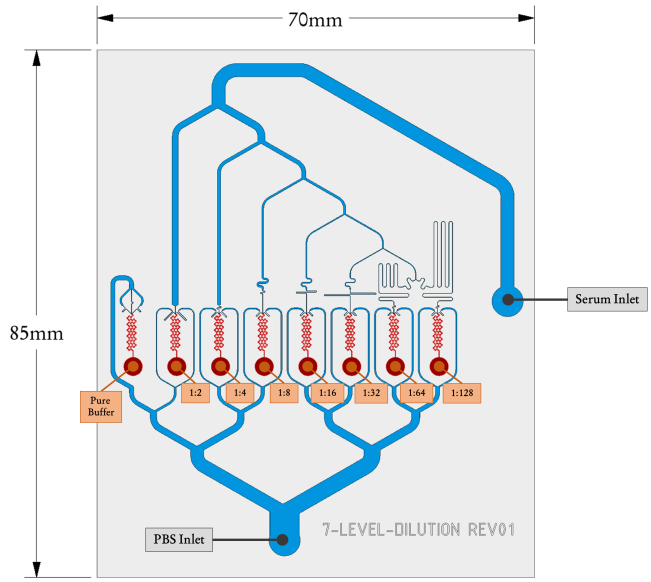

Fig. 14. Layout of 7-dilution microfluidic chip: volume flow rate control networks indicated by blue channels and micromixers indicated by red channels.

2.3 Microfabrication of microfluidic chips

There are two main processes in fabricating a dilution microfluidic chip: the fabrication of the Silicon-master (Si-master) and the casting of the PDMS microfluidic chip. Beginning with the Si-master fabrication, a 6-inch Silicon-wafer (Si-wafer) is cleaned by dipping in a piranha solution in order to remove organic contaminants from the surfaces of Si-wafer. Then, the Si-wafer is spin-coated with the Hexamethyldisilazane (HMDS) and baked at 90° for 90 seconds to improve the photoresist (PR) adhesion to the oxidized Si-wafer surface. A commercially available positive PR, PFI34a (Sumitomo Corporation), is spin-coated at a rate of 1000 rpm for 20 seconds in order to obtain a thickness of approximately 2 µm on the Si-wafer, and the channel patterns are prepared by a conventional photolithography method using a mask aligner (EVG 620, EV Group). The spin-coated wafer is then exposed with 365 nm UV-light through a lithograph mask. The UV-light intensity is 40 mW/cm2 and the exposed time is 5 seconds. A mask with feature sizes ranging from 40 µm to 120 µm is used. The Si-wafer is post-exposure baked at 110° for 100 seconds in order to enhance the hardening of the surface, then developed in SD-W, Sumitomo Corporation, for 75 seconds, and hard baked at 120° for 80 seconds. Afterwards, the photo-patterned Si-wafer is etched via deep reactive ion etcher (DRIE) using SF6/C4F8 gases. The remaining PR is stripped with oxygen plasma. Finally, the Si-master with 40-µm etch depth is obtained. The process schematic of manufacturing the Si-master is displayed in Fig. 15.

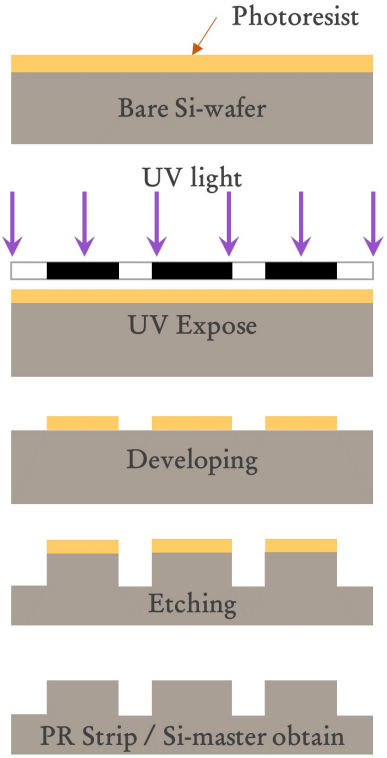

Fig. 15. Silicon-master fabrication process.

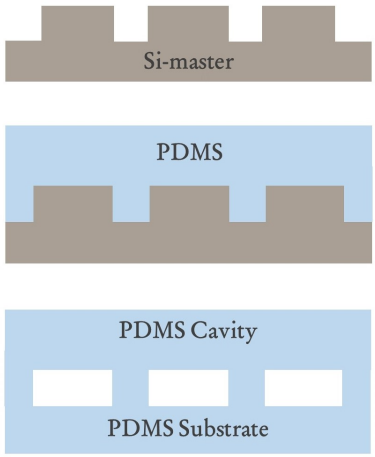

Fig. 16. Molding and attachment process of a microfluidic chip.

Consequently, a Polydimethylsiloxane (PDMS) precursor (Sylgard 184 Silicone Elastomer, Dow Corning) and a curing agent are mixed at a ratio of 10 to 1 by weight. The PDMS mixture is poured onto the Si-master and cured at 75° for 90 min.

Then, the cured PDMS is released from the Si-master, cut and punched to connect silicone tubes. The PDMS cavity side is directly bonded to a PDMS substrate after the surface treatment. The surface treatment is done with oxygen plasma under 40 sccm of O_2 with 30 Watts for 90 seconds. The process schematic of molding and attachment is illustrated in Fig. 16. The prototype of 7-dilution microfluidic chip is shown in Fig. 17.

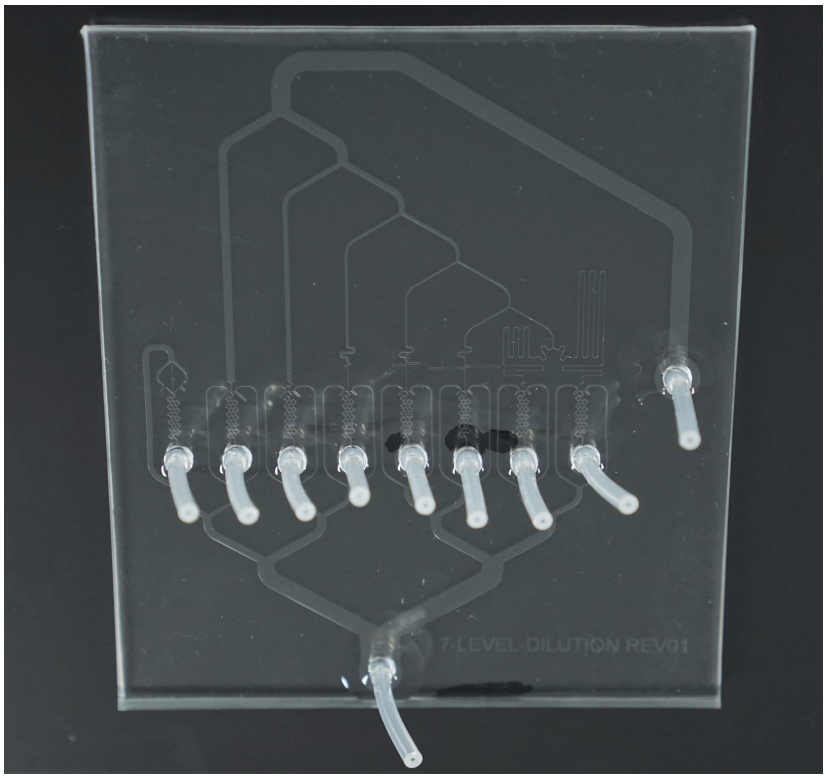

Fig. 17. Prototype of 7-dilution microfluidic chip.

3. Validation

3.1. Design validation of volume concentration ratio with UV-vis absorption method

The protein content in the diluted serum samples can be measured by using the UV-vis Spectrophotometer (Agilent Cary 60 UV-vis) to confirm the volume concentration ratios of the proposed volume flow rates. Pooled serum used in this study is a pooled remnant specimen collected from healthy blood donors at Siriraj hospital. The sample collection protocol was approved by Siriraj Institutional Review Board (approval number SI 330/2016). The standard curve of serum protein can be constructed by preparing various dilutions of serum protein with PBS buffer over the range of 1:75 - 1:1000 dilutions and using the UV absorbance intensity at the wavelength of 280 nm and 1 mL of the diluted serum protein sample, each of which is measured and referred to as amino acids with aromatic rings that absorb ultraviolet light [22-24]. The relation between the absorbance and the concentration is obtained as a linear standard curve for serum, i.e., $A = 0.7799\phi_s$, as shown in Fig. 18 where ϕ_s is the volume concentration of

serum (%) and A is the absorbance of serum [A.U.]. The error of this standard curve is negligible as indicated by R^2 = 0.9999 where R^2 is the coefficient of determination. After that, the UV absorbance of 1 mL of the diluted serum sample from the dilution microfluidic chip is measured and the volume concentration of serum protein that absorbs UV is calculated by using the standard curve obtained so that the protein content in the diluted serum sample is determined. Two syringe pumps (NE-1000, Parkland Scientific, Inc.) are used to feed serum and PBS into the dilution microfluidic chip at the serum and PBS inlets with the volume flow rates of 7.9375 µL/min and 56.0625 µL/min respectively. The volume flow rates used are scaled down 16 times lower than those of the design point in order to fit the capacity of these two syringe pumps.

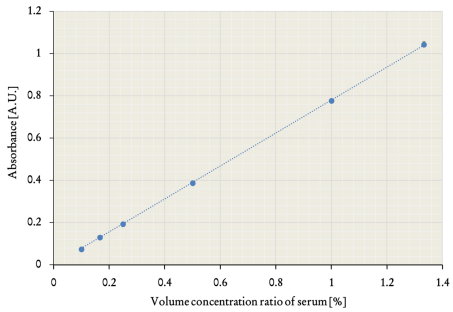

Fig. 18. Standard curve for serum.

Since the volume flow rates and viscosities of serum and PBS are different, the pressure drop in the silicone tube from the syringe pump to the serum inlet must be balanced with the pressure drop in the silicone tube from the syringe pump to the PBS inlet using Eq. (2.25) in Subsection 2.1. As a result, Eq. (2.26) in Subsection 2.1 is obtained. With the measured fluid properties in Table 2 and the feeding volume flow rates of 7.9375 µL/min and 56.0625 µL/min at the serum and PBS inlets, LS = 3.95LP so that the length of the serum silicone tube is 39.5 cm if the length of the PBS silicone tube is 10 cm. The diluted serum sample is obtained at each micromixer outlet as shown in Fig. 19. In order to obtain a sufficient amount of diluted serum samples for UV-vis spectroscopy, the dilution process is operated for 2 hours and 15 minutes: (1) first 15 minutes to purge the whole system of this dilution microfluidic chip and (2) 2 hours to store the diluted serum samples. The measured volume concentration ratios obtained from the UV-vis absorption method are shown in Table 6 where each experimentally averaged volume concentration ratio is obtained by averaging three sets of repeated measurements. In Table 6, the error percentages of seven volume concentration ratios are less than 8% so that the difference between the measured and target volume concentration ratios is in an acceptable range.

Table 6. Measured volume concentration ratios from UV-vis absorption method and target volume concentration ratios.

Volume concentration ratio	Target volume concentration ratio	Experimentally averaged volume concentration ratio	Standard deviation	% Error of volume concentration ratio
1:128	0.0078125	0.008095	0.002925	3.62%
1:64	0.015625	0.016011	0.001330	2.47%
1:32	0.03125	0.032756	0.001474	4.82%
1:16	0.0625	0.064195	0.001261	2.71%
1:8	0.125	0.131278	0.002072	5.02%
1:4	0.25	0.260658	0.003083	4.26%
1:2	0.5	0.536180	0.004520	7.24%

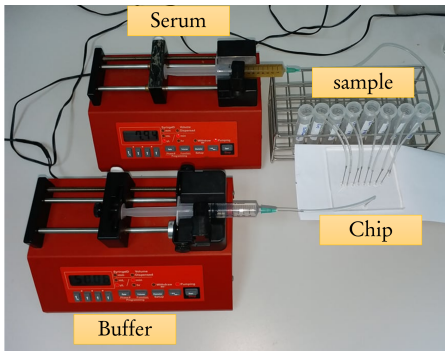

Fig. 19. System of dilution microfluidic chip operation.

3.2. Dilution test of MOG-IgG detection

3.2.1. Preparation of cell culture microfluidic chip

The cell expressing Myelin Oligodendrocyte Glycoprotein (MOG) is cultured in the microfluidic chip. Before cell seeding, the PDMS microfluidic chip is modified by poly-L-lysine as described in our previous study [25, 26]. Then, the microfluidic chip is washed with 200 µl phosphate buffer saline (PBS) pH 7.4. The target cells of 3-5 × 106 cells/ml of Dulbecco's Modified Eagle Medium (DMEM) with 10% fetal bovine serum (FBS) supplementation are fed into the microfluidic chip inlets. The cells in the microfluidic chip are incubated for 48 hours in a moist chamber at 37°C with 5% CO_2.

The cells in the microfluidic chip are then washed for 15 minutes by PBS pH 7.4. The cells are fixed with 4% paraformaldehyde for 30 minutes, washed with 0.1% tween 20 in PBS buffer, permeabilized with 0.5% triton X-100 in PBS buffer for 30 minutes, and washed with PBS buffer for 15 minutes. The cells are incubated with 5% bovine serum albumin in 0.1% tween 20 for at least 1 hour to block non-specific antibody binding.

3.2.2. Artificial serum sample preparation

The serum sample in this study is a pool of the leftover sera collected from at least 50 healthy blood donors who attend the blood donation at Department of Transfusion Medicine, Siriraj Hospital. All sample collections are processed by appropriate sample management protocol approval from Siriraj Institutional Review Board (approval number SI 330/2016). The serum sample is centrifuged at 10,000 g for 10 minutes. Rabbit anti-human MOG immunoglobulin G (MOG-IgG) is added into the serum sample to obtain 1:1,000 titer of MOG-IgG in the PBS.

3.2.3. Cell-based immunofluorescence staining

The parallel dilution microfluidic chip is connected to the cell culture microfluidic chip for cell-based immunofluorescence staining as demonstrated in Fig. 20. The serum and the PBS buffer with the flow rates of 7.94 and 56.06 µl/min are fed respectively into the serum and PBS inlets for 30 minutes. The sample is incubated in the microfluidic chip for 1 hour. The cells in the microfluidic chip are washed for 15 minutes, stained with Alexa Fluor 555 and conjugated to the antibody to detect rabbit IgG. Nuclei of the cells are stained for 5 minutes with 1 µg/ml 4', 6-Diamidino-2-Phenylindole, Dihydrochloride (DAPI) and washed with PBS buffer for 15 minutes. Each microfluidic microchannel is filled with glycerol before collecting the fluorescence images under the fluorescence microscope at 100x magnification. The fluorescence images of the cells in each field of view are captured via blue and red filter cubes of the fluorescence microscope.

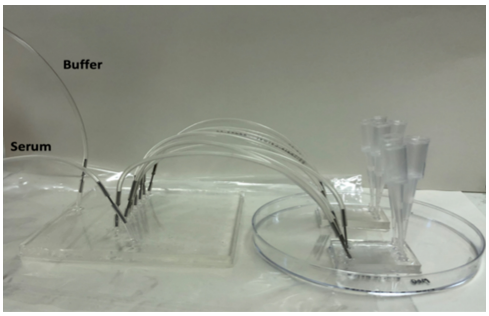

Fig. 20. Microfluidic chip setup composed of a parallel dilution microfluidic chip and a cell culture microfluidic chip used for the evaluation of cell-based immunofluorescence staining protocol.

3.2.4. Fluorescence image analysis

The location of the individual cell is observed from DAPI nuclear staining. The cells are arbitrarily cropped to obtain at least 200 cell images in each channel. Mean fluorescence intensity (MFI) of the red fluorescence signal in each cell is determined regarding their grayscale level (8-bit grayscale image; black (0) – white (225)) by using ImageJ 1.44 image analyzer program [27]. Averaged red MFIs of the cells in each channel are plotted as shown in Fig. 21.

3.2.5. Results of cell-based immunofluorescence staining

Fig. 21 demonstrates the averaged immunostaining signals of the cells that are stained by different titers of rabbit anti-human MOG varying from 0-1:128 MOG-IgG in the PBS buffer. The result shows that the positive correlation of the immunofluorescence staining signal responds to different MOG-IgG titers that are semi-automatically provided by the parallel dilution microfluidic chip.

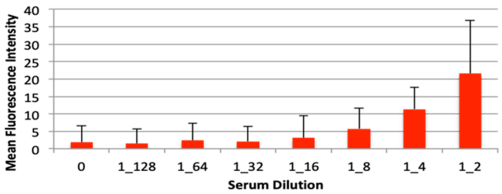

Fig. 21. Averaged MFIs showing the immunofluorescence signal response to different titers of MOG-IgG in the PBS buffer varying from 0 - 1:128.

4. Conclusion

The multiple dilution-in-parallel PDMS microfluidic chip is designed using Hagen-Poiseuille's law and CFD. The volume flow rate control networks are designed to precisely deliver serum and PBS to micromixers. Pressure drops of the volume flow rate control networks are precisely balanced using Hagen–Poiseuille's law, based on the measured fluid properties of serum, PBS buffer, and their mixtures. To obtain the homogeneous mixture achieving the mixing index of 0.96328 - 0.98399 at micromixer outlets, the serpentine microchannel is designed in order to continually generate the Dean vortices for effective mixing. The proposed 7-dilution microfluidic chip can simultaneously deliver the mixture of serum and PBS buffer at seven volume concentration ratios with the high level of homogeneity. This dilution chip with seven serpentine micromixing channels can deliver 1:2 up to 1:128 volume concentration ratio in parallel. The volume concentration ratios obtained at micromixer outlets are in good agreement with the measured ones by the UV-vis absorption method with the maximum error of 7.24%. As tested with MOG-IgG, the cell signals are clearly detected at seven volume concentration ratios. In the future, the detailed CFD simulation of the 7-dilution microfluidic chip starting from the volume flow rate control networks to the outlet of the micromixer is of interest. Moreover, the design of the multiple dilution-in-parallel

PDMS microfluidic chip to support more than 7 levels is another interest.

Acknowledgements

The authors would like to gratefully acknowledge Anton Paar GmbH for providing Density Meter DMA 4500M and Automated Micro Viscometer (AMVn) to measure fluid properties during this research work. This project is funded by Thailand's National Science and Technology Development Agency (NSTDA) (Grant No. P-16-50098) and Faculty of Medicine, Siriraj Hospital (Grant No. r015936004). Therdthai Thienthong is grateful for the tuition-fee-waiving scholarship of TGGS, KMUTNB, during his doctoral study. Numfon Khemthongcharoen was supported by a joint grant from the Thailand Research Fund (TRF) and Thailand's National Science and Technology Development Agency (NSTDA) under the Royal Golden Jubilee Ph.D. (RGJPHD) Program (Grant No. PHD/0213/2557). Biological materials provided by Mr. Nutthapon Yookong are greatly appreciated. Last, but not least, the authors would like to thank Thai Microelectronics Center (TMEC) for fabricating Si master and PDMS casting in addition to the microfluidic chips used in the studies.

References

[1] Rubenstein DA, Yin W, Frame MD. Biofluid mechanics. Elsevier; 2015.

[2] Dixit CK, Kaushik A. Microfluidics for biologists. Springer International Publishing; 2016.

[3] Ottino JM, Wiggins S. Introduction: mixing in microfluidics. Philos Trans R Soc London Ser A Math Phys Eng Sci 2004;362:923-35.

[4] Nguyen N-T, Wu Z. Micromixers – A review. J Micromechanics Microengineering 2005;15:R1-16.

[5] Hessel V, Löwe H, Schönfeld F. Micromixers – a review on passive and active mixing principles. Chem Eng Sci 2005;60:2479-501.

[6] Ward K, Fan ZH. Mixing in microfluidic devices and enhancement methods. J Micromechanics Microengineering 2015;25:094001.

[7] Lee CY, Wang WT, Liu CC, Fu LM. Passive mixers in microfluidic systems: a review. Chem Eng J 2016;288:146-60.

[8] Stroock AD. Chaotic mixer for microchannels. Science 2002;295: 647-51.

[9] Dean WR. LXXII. The stream-line motion of fluid in a curved pipe (Second paper). London, Edinburgh, Dublin Philos Mag J Sci 1928;5:673-95.

[10] Jain S, Unni HN. Numerical modeling and experimental validation of passive microfluidic mixer designs for biological applications. AIP Adv 2020;10.

[11] Usefian A, Bayareh M. Numerical and experimental investigation of an efficient convergent-divergent micromixer. Meccanica 2020;55:1025-35.

[12] Kwon B, Kim JH. Importance of molds for nanoimprint lithography: hard, soft, and hybrid molds. J Nanosci 2016;2016:1-12.

[13] Atthi N, Sripumkhai W, Pattamang P, Thongsook O, Srihapat A, Meananeatra R, et al. Fabrication of robust PDMS micro-structure with hydrophobic and antifouling properties. Microelectron Eng 2020;224:111255.

[14] Angelescu DE. Highly integrated microfluidics design. Artech House; 2011.

[15] Thienthong T, Juntasaro E, Sripumkhai W, Houngkamhang N, Chanasakulniyom M, Khemthongcharoen N, et al. Design

and validation of a multiple dilution microfluidic chip for a human serum preparation. 7th Thai Soc. Mech. Eng. - Int. Conf. Mech. Eng., 2016.

[16] Thienthong T, Juntasaro E, Sripumkhai W, Houngkamhang N, Chanasakulniyom M, Khemthongcharoen N, et al. Mixing-performance evaluation of a multiple dilution microfluidic chip for a human serum dilution process. Eng J 2021;25:67-87.

[17] Bird RB, Lightfoot EN, Stewart WE. Transport phenomena. John Wiley & Sons; 2002.

[18] Wilke CR, Chang P. Correlation of diffusion coefficients in dilute solutions. AIChE J 1955;1:264-70.

[19] National Center for Biotechnology Information. Phosphate-buffered saline information [Internet]. [cited 2020 Sep 24]. Available from: https://pubchem.ncbi.nlm.nih.gov/compound/24978514

[20] Sigma-Aldrich. Human albumin [Internet]. [cited 2020 Sep 24]. Available from: https://www.sigmaaldrich.com/life-science/metabolomics/enzyme-explorer/enzyme-reagents/human-albumin.html

[21] White FM. Viscous fluid flow. McGraw-Hill Education; 2006.

[22] Layne E. Spectrophotometric and turbidimetric methods for measuring proteins. Methods Enzymol., vol. 3, 1957, p. 447-54.

[23] Walker JM. The protein protocols handbook. Humana Press Inc.; 2002.

[24] Upstone SL. Ultraviolet/visible light absorption spectrophotometry in clinical chemistry. Encycl. Anal. Chem., Chichester, UK: John Wiley & Sons, Ltd; 2006, p. 1-15.

[25] Khemthongcharoen N, Uawithya P, Chanasakulniyom M, Yasawong M, Jeamsaksiri W, Sripumkhai W, et al. Polydimethylsiloxane (PDMS) microfluidic modifications for cell-based immunofluorescence assay. J Adhes Sci Technol 2021;35:955-72.

[26] Khemthongcharoen N, Uawithya P, Yookong N, Chanasakulniyom M, Jeamsaksiri W, Sripumkhai W, et al. Microfluidic system evaluation for the semi-automatic detection of MOG-IgG in serum samples. Sens Bio-Sensing Res 2021;34:100458.

[27] Abràmoff MD, Magalhães PJ, Ram SJ. Image processing with imageJ. Biophotonics Int 2004;11:36-41.